Spherical perfect lens: Solutions of Maxwell's equations for spherical geometry

S. Anantha Ramakrishna
Department of Physics, Indian Institute of Technology, Kanpur 208016, India

J. B. Pendry
The Blackett Laboratory, Imperial College London, London SW2 2AZ, United Kingdom

(Received 13 November 2003; published 22 March 2004)

It has been recently proved that a slab of negative refractive index material acts as a perfect lens in that it makes accessible the subwavelength image information contained in the evanescent modes of a source. Here we elaborate on perfect lens solutions to spherical shells of negative refractive material where magnification of the near-field images becomes possible. The negative refractive materials then need to be spatially dispersive with $\varepsilon(r)\sim 1/r$ and $\mu(r)\sim 1/r$. We concentrate on lenslike solutions for the extreme near-field limit. Then the conditions for the TM and TE polarized modes become independent of μ and ε, respectively.

DOI: 10.1103/PhysRevB.69.115115 PACS number(s): 78.20.Ci, 42.30.Wb, 78.45.+h

I. INTRODUCTION

The possibility of a perfect lens[1] whose resolution is not limited by the classical diffraction limit has been subject to intense debate by the scientific community during the past two years. This perfect lens could be realized by using a slab of material with $\varepsilon=\mu=-1$ where ε is the dielectric constant and the μ is the magnetic permeability. Veselago had observed[2] that such a material would have a negative refractive index of $n=-\sqrt{\varepsilon\mu}=-1$ (the negative sign of the square root needs to be chosen by requirements of causality), and a slab of such a material would act as a lens in that it would refocus incident rays from a point source on one side into a point on the other side of the slab (see Fig. 1). Due to the unavailability of materials with simultaneously negative ε and μ, negative refractive index remained an academic curiosity until recently when it became possible to fabricate structured metamaterials that have negative ϵ and μ.[3–5] Most of the negative refractive materials (NRM), so far, consist of interleaving arrays of thin metallic wires [that provide negative ε (Ref. 6)] and metallic split-ring resonators [that provide negative μ (Ref. 7)]. Although some initial concerns were expressed[8] that the observed effects in these experiments were dominated by absorption, the recent experiments of Refs. 9–12 have confirmed that negative refractive materials are today's reality.

It was demonstrated by one of us that the NRM slab acts as a lens not only for the propagating waves (for which the ray analysis of Veselago is valid) but also for the evanescent near-field radiation.[1] This phenomenon of perfect lensing becomes possible due to the surface plasmon states[13] that reside on the surfaces of the NRM slab which restore the amplitudes of the decaying evanescent waves.[1,14–18] Indeed, it has been confirmed by numerical (FDTD) simulations that an incident pulse is temporarily trapped at the interfaces for a considerable time.[19] For a detailed description of the perfect slab lens, we refer the reader to Refs. 1,17,20. The ''perfectness'' of the perfect lens is limited only by the extent to which the constituent NRM are perfect with the specified material parameters. Absorption in the NRM and deviations of the material parameters from the resonant surface plasmon conditions of the perfect lens causes significant degradation of the subwavelength resolution possible.[14,21–23] We have suggested some possible measures to ameliorate this degradation of the lens resolution by stratifying the lens medium[24] and introducing optical gain into the system.[25] It appears that obtaining negative refractive materials with sufficiently low levels of dissipation will be the greatest challenge. We note that although the phenomenon of subwavelength focusing using NRM is yet to be experimentally demonstrated, there is some experimental evidence for the amplification of evanescent waves[26] and we expect that there are good chances for realizing this using NRM at microwave frequencies.

The image formed by the NRM slab lens is identical to the object and hence there is no magnification in the image. Lenses are mostly used to produce magnified or demagnified images and the lack of any magnification is a great restriction on the slab lens on which most of the attention in the literature has been focused. The slab lens is invariant in the transverse directions and conserves the parallel component of the wave vector. To cause magnification this transverse

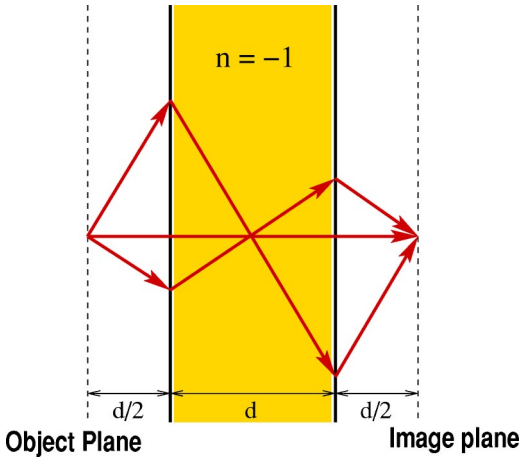

FIG. 1. Radiation from a point source on one side of a slab of material with $i\varepsilon=-1$ and $\mu=-1$ is refocused into a point on the other side. The rays representing propagating waves are bent on to the other side of the normal at the interfaces due to the negative refractive index of the slab.

invariance will have to be broken and curved surfaces necessarily have to be involved. The perfect lens effect is dependent on the near degeneracy of the surface plasmon resonances to amplify the near field, and curved surfaces in general have completely different surface plasmon spectrum.[27] It was recently pointed out by us that a family of near-field lenses (in the quasistatic approximation) in two dimensions can be generated by a conformal mapping of the slab lens.[20] Thus, a cylindrical annulus with dielectric constant $\varepsilon=-1$ was shown to have a lens-like property of projecting in and out images of charge distributions. Similarly in Refs. 28 and 29, it was shown how a general method of coordinate transformations could be used to map the perfect slab lens solution for the Maxwell's equations into a variety of situations including the cylindrical and spherical geometries, respectively.

In this paper, we elaborate on the perfect lens solutions in the spherical geometry and show that media with spatially dispersive dielectric constant $\varepsilon(\vec{r})\sim 1/r$ and magnetic permeability $\mu(\vec{r})\sim 1/r$ can be used to fabricate a spherical perfect lens that can magnify the near-field images as well. In Sec. II of this paper, we will present these perfect lens solutions of the Maxwell's equations for the spherical geometry. In Sec. III, we will examine the solutions in the extreme near-field limit or the quasistatic limit which is useful when the length scales in the problem are all much smaller than a wavelength. Then the requirements for TM and TE polarizations depend only on $\varepsilon\sim 1/r^2$ or $\mu\sim 1/r^2$, respectively. This is useful at frequencies where we are able to generate structures with only one of ε or μ negative. We will investigate the effects of dissipation in the NRM and point out the connections to the one-dimensional (1D) slab lens solutions. We will present our concluding remarks in Sec. IV.

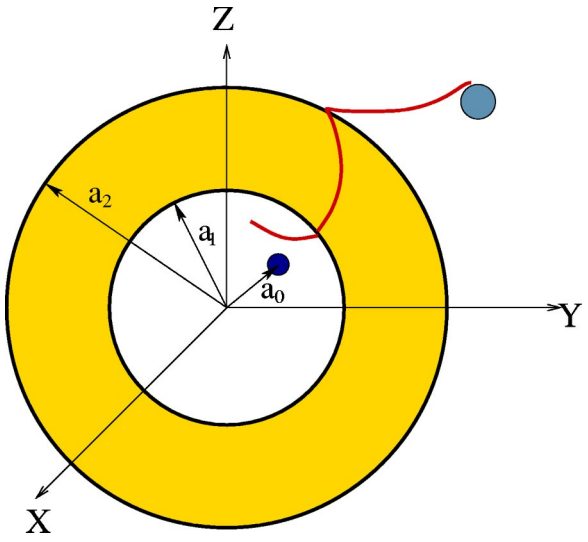

FIG. 2. A spherical shell with negative $\varepsilon_-(r)\sim -1/r$ and $\mu_-(r)\sim -1/r$ images a source located inside the shell into the external region. The media outside have positive refractive index, but $\varepsilon_-(r)\sim 1/r$ and $\mu_-(r)\sim 1/r$. The amplification inside the spherical shell of the otherwise decaying field is schematically shown.

II. A PERFECT SPHERICAL LENS

Consider a spherically symmetric system shown in Fig. 2 consisting of a spherical shell of NRM with the dielectric constant $\varepsilon_-(r)$ and $\mu_-(r)$ imbedded in a positive refractive material with $\varepsilon_+(r)$ and $\mu_+(r)$. First of all we will find the general solutions to the field equations with spatially inhomogeneous material parameters:

$$\nabla\times\mathbf{E}=i\omega\mu_0\mu(\mathbf{r})\mathbf{H}, \qquad \nabla\times\mathbf{H}=-i\omega\varepsilon_0\varepsilon(\mathbf{r})\mathbf{E} \tag{1}$$

$$\nabla\cdot\mathbf{D}=0, \qquad \nabla\cdot\mathbf{H}=0, \tag{2}$$

$$\mathbf{D}=\varepsilon(\mathbf{r})\mathbf{E}, \qquad \mathbf{B}=\mu(\mathbf{r})\mathbf{H}. \tag{3}$$

Under these circumstances of spherical symmetry, it is sufficient to specify the quantities $(\mathbf{r}\cdot\mathbf{E})$ and $(\mathbf{r}\cdot\mathbf{H})$ which will constitute a full solution to the problem. Let us now look at the TM polarized modes $\mathbf{r}\cdot\mathbf{H}=0$, implying that only the electric fields have a radial component E_r. Operating on Eq. (1) by ∇, we have

$$\nabla\times\nabla\times\mathbf{E}=i\omega\mu_0\nabla\times[\mu(\mathbf{r})\mathbf{H}],$$

$$=\frac{\omega^2}{c^2}\mu(\mathbf{r})\varepsilon(\mathbf{r})\mathbf{E}+i\omega\frac{\nabla\mu(\mathbf{r})}{\mu(\mathbf{r})}\times\nabla\times\mathbf{E}. \tag{4}$$

Using Eqs. (2) and (3) we have

$$\nabla\cdot\mathbf{D}=\nabla\cdot[\varepsilon(\mathbf{r})\mathbf{E}]=\nabla\varepsilon(\mathbf{r})\cdot\mathbf{E}+\varepsilon(\mathbf{r})\nabla\cdot\mathbf{E}=0, \tag{5}$$

and if we assume $\varepsilon(\mathbf{r})=\varepsilon(r)$ and $\mu(\mathbf{r})=\mu(r)$, we have

$$\nabla\cdot\mathbf{E}=-\frac{\varepsilon'(r)}{r\varepsilon(r)}\mathbf{r}\cdot\mathbf{E}=-\frac{\varepsilon'(r)}{r\varepsilon(r)}(rE_r). \tag{6}$$

We note the following identities for later use:

$$\nabla\times\nabla\times\mathbf{E}=\nabla(\nabla\cdot\mathbf{E})-\nabla^2\mathbf{E}, \tag{7}$$

$$\nabla^2(\mathbf{r}\cdot\mathbf{E})=\mathbf{r}\cdot\nabla^2\mathbf{E}+2\nabla\cdot\mathbf{E}, \tag{8}$$

and using Eq. (6) we also note that

$$\begin{aligned}\mathbf{r}\cdot\nabla(\nabla\cdot\mathbf{E})&=\mathbf{r}\cdot\nabla\left(-\frac{\varepsilon'(r)}{\varepsilon(r)}E_r\right),\\&=-r\frac{\partial}{\partial r}\left(\frac{\varepsilon'(r)}{\varepsilon(r)}E_r\right),\\&=-\frac{\partial}{\partial r}\left(\frac{\varepsilon'(r)}{\varepsilon(r)}(rE_r)\right)\\&\quad+\left(\frac{\varepsilon'(r)}{\varepsilon(r)}E_r\right).\end{aligned} \tag{9}$$

We now take a dot product of $\mathbf{r}$ with Eq. (4), and use the Eqs. (6)–(9) to get an equation for (rE_r) as:

$$\nabla^2(rE_r)+\frac{\partial}{\partial r}\left[\frac{\varepsilon'(r)}{\varepsilon(r)}(rE_r)\right]+\frac{\varepsilon'(r)}{r\varepsilon(r)}(rE_r)$$

$$+\varepsilon(r)\mu(r)\frac{\omega^2}{c^2}(rE_r)=0. \tag{10}$$

This equation is separable and the spherical harmonics are a solution to the angular part. Hence the solution is $(rE_r) = U(r)Y_{lm}(\theta,\phi)$, where the radial part $U(r)$ satisfies

$$\frac{1}{r^2}\frac{\partial}{\partial r}\left(r^2\frac{\partial U}{\partial r}\right) - \frac{l(l+1)}{r^2}U + \frac{\partial}{\partial r}\left[\frac{\varepsilon'(r)}{\varepsilon(r)}U\right] + \frac{\varepsilon'(r)}{r\varepsilon(r)}U + \varepsilon(r)\mu(r)\frac{\omega^2}{c^2}U = 0. \tag{11}$$

If we choose $\varepsilon(r)=\alpha r^p$ and $\mu(r)=\beta r^q$, we can have a solution $U(r)\sim r^n$ and we get

$$[n(n+1)-l(l+1)+p(n-1)+p]r^{n-2} + \alpha\beta\omega^2/c^2 r^{p+q+n} = 0, \tag{12}$$

implying $p+q=-2$ and

$$n_\pm = \tfrac{1}{2}[-(p+1)\pm\sqrt{(p+1)^2+4l(l+1)-4\alpha\beta\omega^2/c^2}]. \tag{13}$$

Hence the general solution can be written as

$$E_r(\mathbf{r}) = \sum_{l,m}[n_+A_{lm}r^{n_+-1}+n_-B_{lm}r^{n_--1}]Y_{lm}(\theta,\phi). \tag{14}$$

A similar solution can be obtained for the TE modes with $\mathbf{r}\cdot\mathbf{E}=0$.

Now assuming an arbitrary source at $r=a_0$, we can now write down the electric fields of the TM modes in the different regions for the negative spherical shell of Fig. 2 as

$$\mathbf{E}^{(1)}(\mathbf{r}) = \sum_{l,m}[n_+A^{(1)}_{lm}r^{n_+-1}+n_-B^{(1)}_{lm}r^{n_--1}]Y_{lm}(\theta,\phi), \quad a_0<r<a_1, \tag{15}$$

$$\mathbf{E}^{(2)}(\mathbf{r}) = \sum_{l,m}[n_+A^{(2)}_{lm}r^{n_+-1}+n_-B^{(2)}_{lm}r^{n_--1}]Y_{lm}(\theta,\phi), \quad a_1<r<a_2, \tag{16}$$

$$\mathbf{E}^{(3)}(\mathbf{r}) = \sum_{l,m}[n_+A^{(3)}_{lm}r^{n_+-1}+n_-B^{(3)}_{lm}r^{n_--1}]Y_{lm}(\theta,\phi), \quad a_2<r<\infty, \tag{17}$$

and similarly for the magnetic fields. Note that $B^{(1)}_{lm}$ correspond to the field components of the source located at $r=a_0$. For causal solutions $A^{(3)}_{lm}=0$. Now the tangential components of the magnetic fields and the normal components of the displacement fields have to be continuous across the interfaces. Under the conditions $p=-1$, $q=-1$, $\varepsilon_+(a_1)=-\varepsilon_-(a_1)$, and $\varepsilon_+(a_2)=-\varepsilon_-(a_2)$, we have

$$A^{(1)}_{lm}=0, \tag{18}$$

$$A^{(2)}_{lm}=\left(\frac{1}{a_1^2}\right)^{\sqrt{l(l+1)-\alpha\beta\omega^2/c^2}} B^{(1)}_{lm}, \tag{19}$$

$$B^{(2)}_{lm}=0, \tag{20}$$

$$B^{(3)}_{lm}=\left(\frac{a_2^2}{a_1^2}\right)^{\sqrt{l(l+1)-\alpha\beta\omega^2/c^2}} B^{(1)}_{lm}. \tag{21}$$

The lenslike property of the system becomes clear by writing the field outside the spherical shell as

$$E^{(3)}_r=\frac{1}{r}\left[\frac{a_2^2}{a_1^2}r\right]^{\sqrt{l(l+1)-\alpha\beta\omega^2/c^2}} B^{(1)}_{lm}Y_{lm}(\theta,\phi). \tag{22}$$

Hence apart from a scaling factor of $1/r$, the fields on the sphere $r=a_3=(a_2^2/a_1^2)a_0$ are identical to the fields on the sphere $r=a_0$. There is also a spatial magnification in the image by a factor of a_2^2/a_1^2.

Let us note a couple of points about the above perfect lens solutions in the spherical geometry. First, for $r>a_3$, i.e., points outside the image surface the fields appear as if the source were located on the spherical image surface ($r=a_3$). However, this is not true for points $a_2<r<a_3$ within the image surface. Second, given that $\varepsilon_-(a_2)=-\varepsilon_+(a_2)$, we have the perfect lens solutions if and only if $n_+=-n_-$ which implies that $p=-1$ in Eq. (13). Although the solutions given by Eq. (14) occur in any medium with $\varepsilon\mu\sim 1/r^2$, the perfect lens solutions only occur for $\varepsilon\sim\mu\sim 1/r$. Here we have written down the solutions for the TM modes. The solutions for the TE modes can be similarly obtained.

III. THE SPHERICAL NEAR-FIELD LENS

As it has been pointed out in the preceding section, the "power" solutions are good for any $\varepsilon(r)\sim r^p$ and $\mu(r)\sim r^q$ such that $p+q=-2$. However, the perfect lens solutions for the Maxwell's equations result only for the single case of $p=q=-1$. In the quasistatic limit of $\omega\to 0$ and $l\gg|p|$, $|q|$, we can relax this condition. In particular, by setting $\varepsilon(r)\sim 1/r^2$ and $\mu(r)=$ constant, we can have a perfect lens for the TM modes alone. Similarly, we can have a perfect lens for the TE polarization by having $\mu\sim 1/r^2$ and $\varepsilon=$constant.

This extreme near-field limit is both important and valid for situations when all length scales in the problem are much smaller than a wavelength of the radiation. This becomes useful at frequencies where we can only generate media with either negative ε and positive μ, or, negative μ and positive ε. Examples are the silver slab lens at optical frequencies,[1] the metamaterials (Swiss rolls) used for magnetic resonance imaging at radio frequencies.[30] Particularly at radio and microwave frequencies, we currently can practically engineer the required metamaterials with spatially dispersive characteristics at the corresponding length scales. Further it also lifts the restriction that the system has to have a spatially dispersive material parameters even outside the spherical

shell of NRM. In this section we will work in this extreme near-field limit. Then it is sufficient to solve the Laplace equation and we present lenslike solutions to the Laplace equation below.

Consider the spherical shell in Fig. 2 to be filled with a material with $\epsilon_2(r) \sim -C/r^2$ with the inner and outer regions filled with constant dielectrics of ε_1 and ε_3, respectively. Let $\mu=1$ everywhere. Now place a charge $+q$ at the center of the concentric spheres and a charge $-q$ at a distance a_0 from the center inside region 1. We will consider the z axis to be along the dipole axis and make use of the azimuthal symmetry here, although it is clear that our results do not depend on any such assumption of azimuthal symmetry. Thus, all our charge and their images will now lie along the z axis.

Now we will calculate the potentials in the three regions, which satisfies the Laplace equation and the continuity conditions at the interfaces. The potential in region 1 ($r<a_1$) can be calculated to be (using the azimuthal symmetry)

$$V_1(\mathbf{r}) = \frac{-q}{4\pi\epsilon_1} \sum_{l=1}^{\infty} \left[A_{1l} r^l P_l(\cos\theta) + \frac{a_0^l}{r^{l+1}} P_l(\cos\theta) \right]. \tag{23}$$

Note that the second term in the above expansion arises due to the dipole within the sphere. It can be shown (see the Appendix), that the general form of the potential in region 2 ($a_1<r<a_2$) where the dielectric constant varies as $1/r^2$ is

$$V_2(\mathbf{r}) = \frac{-q}{4\pi\epsilon_0} \sum_{l=1}^{\infty} \left[A_{2l} r^{(l+1)} P_l(\cos\theta) + \frac{B_{2l}}{r^l} P_l(\cos\theta) \right]. \tag{24}$$

In region 3 ($r>a_2$), the potential is given by

$$V_3(\mathbf{r}) = \frac{-q}{4\pi\epsilon_3} \sum_{l=1}^{\infty} \left[\frac{B_{3l}}{r^{l+1}} P_l(\cos\theta) \right]. \tag{25}$$

Now we must match the potentials at the interfaces at $r=a_1$ and $r=a_2$ (put $\epsilon_0=1$) to determine the A and B coefficients. The conditions of continuity of the potential and the normal component of $\vec{D}$ at the interfaces are

$$V_1(a_1) = V_2(a_1), \qquad V_2(a_2) = V_3(a_2), \tag{26}$$

$$\epsilon_1 \frac{\partial V_1(a_1)}{\partial r} = \epsilon_2 \frac{\partial V_2(a_1)}{\partial r}, \qquad \epsilon_2 \frac{\partial V_2(a_2)}{\partial r} = \epsilon_3 \frac{\partial V_3(a_2)}{\partial r}. \tag{27}$$

We determine the coefficients from these conditions to be

$$A_{1l} = \frac{(l+1)a_0^l \left\{ [l\epsilon_2(a_2) - (l+1)\epsilon_3][\epsilon_1 + \epsilon_2(a_1)] - [\epsilon_2(a_2) + \epsilon_3][(l+1)\epsilon_1 - l\epsilon_2(a_1)] \frac{a_2^{2l+1}}{a_1^{2l+1}} \right\}}{l(l+1)[\epsilon_1 + \epsilon_2(a_1)][\epsilon_2(a_2) + \epsilon_3] a_2^{2l+1} + [l\epsilon_1 - (l+1)\epsilon_2(a_1)][l\epsilon_2(a_2) - (l+1)\epsilon_3] a_1^{2l+1}}, \tag{28}$$

$$A_{2l} = \frac{(2l+1)[l\epsilon_2(a_2) - (l+1)\epsilon_3] a_0^l a_1^{-1}}{l(l+1)[\epsilon_1 + \epsilon_2(a_1)][\epsilon_2(a_2) + \epsilon_3] a_2^{2l+1} + [l\epsilon_1 - (l+1)\epsilon_2(a_1)][l\epsilon_2(a_2) - (l+1)\epsilon_3] a_1^{2l+1}}, \tag{29}$$

$$B_{2l} = \frac{(2l+1)(l+1)[\epsilon_2(a_2) + \epsilon_3] a_2^l a_0^l a_1^{-(l+2)}}{l(l+1)[\epsilon_1 + \epsilon_2(a_1)][\epsilon_2(a_2) + \epsilon_3] a_2^{2l+1} + [l\epsilon_1 - (l+1)\epsilon_2(a_1)][l\epsilon_2(a_2) - (l+1)\epsilon_3] a_1^{2l+1}}, \tag{30}$$

$$B_{3l} = \frac{(2l+1)^2 \epsilon_3 \epsilon_2(a_2) a_0^l a_2^{2(l+1)} a_1^{-1}}{l(l+1)[\epsilon_1 + \epsilon_2(a_1)][\epsilon_2(a_2) + \epsilon_3] a_2^{2l+1} + [l\epsilon_1 - (l+1)\epsilon_2(a_1)][l\epsilon_2(a_2) - (l+1)\epsilon_3] a_1^{2l+1}}. \tag{31}$$

Under the perfect lens conditions

$$\varepsilon_2(a_1) = -\varepsilon_1,$$

and

$$\varepsilon_2(a_2) = -\varepsilon_3, \tag{32}$$

we have

$$A_{1l} = 0, \tag{33}$$

$$A_{2l} = \frac{1}{\varepsilon_1} \frac{a_0^l}{a_1^{2(l+1)}}, \tag{34}$$

$$B_{2l} = 0, \tag{35}$$

$$B_{3l} = \frac{\varepsilon_3}{\varepsilon_1} \left(\frac{a_2}{a_1} \right)^{2(l+1)} a_0^l. \tag{36}$$

Hence the potential outside the spherical shell for $r>a_2$ is

$$V_3(\vec{r}) = \frac{-q}{4\pi\varepsilon_3} \sum_{l=1}^{\infty} \frac{\varepsilon_3}{\varepsilon_1} \left(\frac{a_2}{a_1}\right)^{2(l+1)} \frac{a_0^l}{r^{l+1}} P_l(\cos\theta), \quad (37)$$

which is the potential of a dipole with the positive charge at the origin and the negative charge at a_3, where

$$a_3 = \left(\frac{a_2}{a_1}\right)^2 a_0 \quad (38)$$

and of strength

$$q_2 = \frac{\varepsilon_3}{\varepsilon_1} \left(\frac{a_2}{a_1}\right)^2 q = q, \quad (39)$$

as $\varepsilon_3/\varepsilon_1 = (a_1/a_2)^2$. Thus, on one side of the image (the region $r > a_3$) the fields of a point charge located at a_3 are reproduced. However, it should be pointed out that there is no physical charge in the image location, and the fields on the other side of the image (i.e., in the region $a_2 < r < a_3$) do not converge to the fields of the object and cannot do so in the absence of a charge in the image. Further there is no change in the strength of the charge either. There is a magnification in the image formed by a factor of $(a_2/a_1)^2$.

Now let us consider the case of a point source placed at a_3 in the outer region. Again assuming the z axis to pass through a_3, we can write the potentials in the three regions as

$$V_1(\mathbf{r}) = \frac{+q}{4\pi\varepsilon_1} \sum_{l=0}^{\infty} A_{1l} r^l P_l(\cos\theta) \quad \forall \quad r < a_1, \quad (40)$$

$$V_2(\mathbf{r}) = \frac{+q}{4\pi} \sum_{l=0}^{\infty} \left[A_{2l} r^{l+1} + \frac{B_{2l}}{r^l} \right] P_l(\cos\theta) \quad \forall \quad a_1 < r < a_2, \quad (41)$$

$$V_3(\mathbf{r}) = \frac{+q}{4\pi\varepsilon_3} \sum_{l=0}^{\infty} \left[\frac{r^l}{a_3^{l+1}} + \frac{B_{3l}}{r^{l+1}} \right] P_l(\cos\theta), \quad \forall \quad a_2 < r < a_3, \quad (42)$$

where the first term in $V_3(\vec{r})$ comes from the point source at a_3. Now applying the conditions of continuity at the interfaces, we can similiarly obtain for the coefficients as before. In the limiting case of $\varepsilon_2(a_1) = -\varepsilon_1$ and $\varepsilon_2(a_2) = -\varepsilon_3$, we have

$$A_{1l} = \frac{\varepsilon_1}{\varepsilon_3} \left(\frac{a_2}{a_1}\right)^{2l} \frac{1}{a_3^{l+1}}, \quad (43)$$

$$A_{2l} = 0, \quad (44)$$

$$B_{2l} = \frac{1}{\varepsilon_3} \frac{a_2^{2l}}{a_3^{2l+1}}, \quad (45)$$

$$B_{3l} = 0. \quad (46)$$

Hence the potential inside the inner sphere is

$$V_1(\mathbf{r}) = \frac{q}{4\pi\varepsilon_1} \sum_{l=0}^{\infty} \frac{\varepsilon_1}{\varepsilon_3} \left(\frac{a_2}{a_1}\right)^{2l} \frac{r^l}{a_3^{l+1}} P_l(\cos\theta), \quad (47)$$

i.e., that of a point charge of strength $q_1 = (\varepsilon_1/\varepsilon_3)(a_1/a_2)^2 = q$ at $a_0 = a_3(a_1/a_2)^2$. As before, for the inner region of $r < a_0$, the system behaves as if there were a single charge of strength q located at $r = a_0$. Thus, the shell has a lenslike action. We note that there is a demagnification of $(a_1/a_2)^2$ in this case.

A. Similarities to the 1D slab lens

Let us point out the similarities to the planar slab lens. In both cases, the electromagnetic field grows in amplitude across the negative medium when the perfect lens conditions are satisfied at the interfaces: as an exponential ($\exp[+k_x z]$) in the planar lens and as a power of the radial distance r^l in the spherical lens. The decaying solution away from the source is absent in the negative medium in both cases. Further, when the perfect lens conditions are matched at both the interfaces, there is no reflected wave in both the planar slab as well as the spherical lens, i.e., the impedance matching is perfect as well. In addition this mapping preserves the strength of the charge.

The key differences, however, are the different dielectric constants on either side of the spherical shell of the negative medium. This is a direct consequence of the spatial $1/r^2$ dependence of the negative dielectric constant which relates the two positive dielectric constants to be $\epsilon_1 = (a_1/a_2)^2 \epsilon_3$. But this need not be a particular restriction as we can use the ideas of the asymmetric lens to terminate the different positive media at some radii beyond.[17] The net result is that the image can now be magnified (or demagnified) when the image of the charge (source) is projected out of (or into) the spherical shell, which is true in the 2D cylindrical lens as well.[20]

B. Possibility of the asymmetric lens

In the case of a planar slab, it was possible to have the perfect lens effect by satisfying the required conditions at any one interface—not necessarily at both interfaces.[17] Particularly, in the limit of very large parallel wave vectors the lensing is indeed perfect, although the image intensity differed from the source by a constant factor. Similarly let us now investigate the effects of having the perfect lens conditions in the case of the spherical lens at only one of the interfaces.

Let us consider first, the case of projecting out the image of a point source from inside the spherical shell to outside and enable the perfect lens conditions only at the outer interface $\epsilon_2(r = a_2) = -\epsilon_3$ and have an arbitrary ϵ_1. Now the A and B coefficients come out to be

$$A_{1l} = \frac{a_0^l}{a_1^{2l+1}} \frac{(l+1)[\varepsilon_1 + \varepsilon_2(a_1)]}{l\varepsilon_1 - (l+1)\varepsilon_2(a_1)}, \quad (48)$$

$$A_{2l}=\frac{(2l+1)a_0^l}{l\varepsilon_1-(l+1)\varepsilon_2(a_1)a_1^{2l+2}}, \tag{49}$$

$$B_{2l}=0, \tag{50}$$

$$B_{3l}=\frac{(2l+1)\varepsilon_3 a_0^l}{l\varepsilon_1(a_1/a_2)^2+(l+1)\varepsilon_3}\left(\frac{a_2}{a_1}\right)^{2l}. \tag{51}$$

Only the growing solution within the negative spherical shell remains. The coefficient of the decaying solution (B_{2l}) remains strictly zero. Thus, amplification of the decaying field at least is possible in this case as well. But there is a finite reflectivity in this case. However, the solution outside for $r>a_2$ is not the exact image field of the point source as the coefficient B_{3l} has an extra dependence on l through the dependence on the dielectric constants. Moreover, the process does not preserve the strength of the charge due to the different dielectric constants involved. This should be compared to the solution of the planar asymmetric slab lens where, at least in the electrostatic limit, the system behaved as a perfect lens. In this case, the system behaves as a spherical asymmetric perfect lens only in the limit of large $l\to\infty$. The solution outside the spherical shell is the same when we meet the perfect lens condition on the inner interface—just as in the case of the planar slab lens. However, the reflection coefficient is again nonzero, but different to the earlier case. In either case, the fields are largest at the interface where one meets the perfect lens conditions or the interface on which the surface plasmons are excited.

C. Effects of dissipation

Media with negative real part of the dielectric constant are absorptive (as all metals are), and hence we can write the dielectric constant $\varepsilon(r)=C/r^2+i\varepsilon_i(r)$ (note that $\varepsilon_i\sim 1/r^2$ as well for us to be able to write the solution in the following form). Consider the first case of projecting out the image of a dipole located within the spherical shell where the potential outside the shell is given by Eq. (25) and B_{3l} is given by Eq. (31). When we have a dissipative negative medium and have the perfect lens conditions at the interfaces on the real parts of the dielectric constant alone, $\varepsilon_2(a_1)=-\varepsilon_1+i\varepsilon_i(a_1)$ and $\varepsilon_2(a_2)=-\varepsilon_3+i\varepsilon_i(a_2)$. In parallel with the case of the planar lens, we note that the denominator of B_{3l} consists of two terms, one containing a power of the (smaller) radius a_1 and the other containing a power of the (larger) radius a_2. Crucially the amplification of the evanescent fields depends on the possibility that the smaller power dominates by making the coefficient of the larger term as close as possible to zero. The presence of the imaginary part of the dielectric constant would not allow the coefficient to be zero and the image restoration is good only as long as the term containing a_1 dominates in the denominator of B_{3l}, i.e.,

$$\begin{aligned} l(l+1)\varepsilon_i(a_1)\varepsilon_i(a_2)a_2^{2l+1} \\ \ll[(2l+1)\varepsilon_1-i(l+1)\varepsilon_i(a_1)][-(2l+1)\varepsilon_3 \\ +i\varepsilon_i(a_2)]a_1^{2l+1}. \end{aligned} \tag{52}$$

Hence a useful estimate of the extent of image resolution can be obtained by noting the multipole l for which the two terms in the denominator are approximately equal.[14] We obtain for this value

$$l_{\max}\simeq\frac{\ln\{3\varepsilon_1\varepsilon_3/[\varepsilon_i(a_1)\varepsilon_i(a_2)]\}}{2\ln(a_2/a_1)}. \tag{53}$$

Higher-order multipoles are essentially unresolved in the image. We can similarly obtain the same criterion by considering the second case of transferring the image of a charge located outside the spherical shell into the inner region. Again, we can consider the effects of deviating from the perfect lens conditions on the real part of the dielectric constant as well and obtain a similar limit for the image resolution due to those deviations.

IV. CONCLUSIONS

In conclusion, we have presented a spherical perfect lens which enables magnification of the near-field images. The perfect lens solution requires media with $\varepsilon(r)\sim 1/r$ and $\mu(r)\sim 1/r$ and the conditions $\varepsilon_-(a_{1,2})=-\varepsilon_+(a_{1,2})$ and $\mu_-(a_{1,2})=-\mu_+(a_{1,2})$ at the interfaces of the spherical shell of the NRM. We have shown that in the quasistatic limit of small frequencies ($\omega\to 0$) and high-order multipoles $l\gg|p|$, this condition can be relaxed and the two polarizations (TE and TM modes) decouple. Thus, a shell with negative dielectric constant $\varepsilon_-(r)\sim -1/r^2$ with $\mu=$constant can act as a near-field lens for the TM polarization while $\mu_-(r)\sim -1/r^2$ with $\varepsilon_-(r)=$constant acts as a near-field lens for the TE modes. We have shown that dissipation in the lens material, however, prevents good resolution of higher-order multipoles. Thus, while the near-field lenses work best for the higher-order multipoles, dissipation cutsoff the higher-order multipoles. Further the spherical lens works in the asymmetric mode only in the limit of high-order multipoles. Thus, one has to find an intermediate regime where dissipation does not wipe out the near-field image information and yet the metamaterials work. This is the design challenge involving these near-field lenses.

APPENDIX: SOLUTION OF THE LAPLACE EQUATION IN A SPATIALLY VARYING MEDIUM

We have to solve the Maxwell equations in material media

$$\nabla\cdot\mathbf{D}=0, \qquad \Rightarrow \qquad \nabla(\varepsilon\mathbf{E})=0. \tag{A1}$$

Using $\mathbf{E}=-\nabla V$, where $V(\mathbf{r})$ is the electrostatic potential we have:

$$\varepsilon(\mathbf{r})\nabla^2 V+\nabla\varepsilon(\mathbf{r})\cdot\nabla V=0. \tag{A2}$$

If $\varepsilon(\mathbf{r})$ has only a radial dependence (as in our case $\sim 1/r^2$), then $\nabla\varepsilon(\mathbf{r})=\hat{r}(\partial\varepsilon/\partial r)$ and we can separate the solution as $V(\mathbf{r})=(U(r)/r)Y_{lm}(\theta,\phi)$, where the Y_{lm} is the spherical harmonic and the radial part $U(r)$ satisfies

$$\varepsilon(r)\frac{d^2U}{dr^2}-\frac{l(l+1)}{r^2}U+\frac{d\varepsilon}{dr}\left[\frac{dU}{dr}-\frac{U}{r}\right]=0. \qquad \text{(A3)}$$

To have a solution as a single power of r, the only choices possible for the dielectric constant are either $\varepsilon=C$, a constant—the usual case, or $\varepsilon=C/r^2$. In the latter case the solution is $U(r)\sim r^{l+2}$ or $U(r)\sim r^{-(l-1)}$. The full solution can then be written as

$$V(\mathbf{r})=\sum_{l=0}^{\infty}[A_{lm}r^{l+1}+B_{lm}r^{-l}]Y_{lm}(\theta,\phi). \qquad \text{(A4)}$$

[1] J.B. Pendry, Phys. Rev. Lett. **85**, 3966 (2000).
[2] V.G. Veselago, Usp. Fiz. Nauk **92**, 517 (1964) [Sov. Phys. Usp. **10**, 509 (1968)].
[3] D.R. Smith, W.J. Padilla, D.C. Vier, S.C. Nemat-Nasser, and S. Schultz, Phys. Rev. Lett. **84**, 4184 (2000).
[4] R.A. Shelby, D.R. Smith, and S. Schultz, Science **292**, 77 (2001).
[5] A. Grbic and G.V. Eleftheriades, J. Appl. Phys. **92**, 5930 (2002).
[6] J.B. Pendry, A.J. Holden, W.J. Stewart, and I. Youngs, Phys. Rev. Lett. **76**, 4773 (1996); J.B. Pendry, A.J. Holden, D.J. Robbins, and W.J. Steward, J. Phys.: Condens. Matter **10**, 4785 (1998).
[7] J.B. Pendry, A.J. Holden, D.J. Robbins, and W.J. Steward, IEEE Trans. Microwave Theory Tech. **47**, 2075 (1999).
[8] N. Garcia and M. Nieto-Vesperinas, Opt. Lett. **27**, 885 (2002).
[9] C.G. Parazzoli, R.B. Greegor, K. Li, B.E.C. Kotenbah, and M. Tanielan, Phys. Rev. Lett. **90**, 107401 (2003).
[10] A.A. Houck, J.B. Brock, and I.L. Chuang, Phys. Rev. Lett. **90**, 137401 (2003).
[11] A. Grbic and G.V. Eleftheriades, Appl. Phys. Lett. **82**, 1815 (2003).
[12] P.V. Parimi, W.T. Lu, P. Vodo, J. Sokoloff, and S. Sridhar, cond-mat/0306109 (unpublished).
[13] H. Raether, *Surface Plasmons* (Springer-Verlag, Berlin, 1988).
[14] D.R. Smith, D. Schurig, M. Rosenbluth, S. Schultz, S.A. Ramakrishna, and J.B. Pendry, Appl. Phys. Lett. **82**, 1506 (2003).
[15] F.D.M. Haldane, cond-mat/0206420 (unpublished).
[16] G. Gomez-Santos, Phys. Rev. Lett. **90**, 077401 (2003).
[17] S.A. Ramakrishna, J.B. Pendry, D.R. Smith, D. Schurig, and S. Schultz, J. Mod. Opt. **49**, 1747 (2002)
[18] X.S. Rao and C.N. Ong, Phys. Rev. B **68**, 113103 (2003).
[19] S. Foteinopolou, E.N. Economou, and C.M. Soukoulis, Phys. Rev. Lett. **90**, 107402 (2003).
[20] J.B. Pendry and S.A. Ramakrishna, J. Phys.: Condens. Matter **14**, 8463 (2002).
[21] J.T. Shen and P. Platzmann, Appl. Phys. Lett. **90**, 3286 (2002)
[22] Z. Ye, Phys. Rev. B **67**, 193106 (2003).
[23] N. Fang and X. Zhang, Appl. Phys. Lett. **82**, 161 (2003).
[24] S.A. Ramakrishna, J.B. Pendry, M.C.K. Wiltshire, and W.J. Stewart, J. Mod. Opt. **50**, 1419 (2003).
[25] S.A. Ramakrishna and J.B. Pendry, Phys. Rev. B **67**, 201101(R) (2003).
[26] Z. Liu, N. Fang, T-J. Yen, and X. Zhang, Appl. Phys. Lett. **83**, 5184 (2003).
[27] V.V. Klimov, Opt. Commun. **211**, 183 (2002).
[28] J.B. Pendry, Opt. Express **11**, 755 (2003).
[29] J.B. Pendry and S.A. Ramakrishna, J. Phys.: Condens. Matter **15**, 6345 (2003)
[30] M.C.K. Wiltshire, J.B. Pendry, I.R. Young, D.J. Larkman, D.J. Gilderdale, and J.V. Hajnal, Science **291**, 848 (2001); Opt. Express **11**, 709 (2003).